AISI-1020 Low-carbon Steel Outgassing Analysis

A report submitted in partial fulfillment of the requirement
for the degree of Bachelor of Science in
Physics from the College of William and Mary in Virginia,

by

Hantao Yu

Advisor: Prof. William Cooke

Williamsburg, Virginia
May 19 2022

Contents

Acknowledgments

I would like to thank my supervisor, Prof. William Cooke, for his helpful instructions through each stage of the process. I learned a lot from his instructions, including the serious and cautious attitude towards every detail. I really cannot reach this far without his help. I also would like to thank Prof. David Armstrong for his instructions on how to conduct a research and how to write a scientific report properly.

List of Figures

List of Tables

Abstract

The proposed Cosmic Explorer, an extended version of the LIGOS gravity wave detectors, will require high vacuum spectrometer arms that are at least 10 kilometers long. The use of low carbon steel, instead of the stainless steel used in LIGOS, could reduce the Cosmic Explorer construction costs by as much as 100 million dollars. One promising example, AISI-1020, has been shown to release only 0.1 percent of the gases released by stainless steel under high vacuum. This reduced outgassing could improve the spectrometer performance. We are using a Residual Gas Analyzer (RGA) to characterize the constituent gases released after this steel has been exposed to atmosphere. The gas composition changes when it enters the RGA chamber, so we have developed a pulsed analysis technique. This project is developing numerical techniques to model and to eliminate background signals and then to extract the original gas composition from the pulsed measurement data. Our preliminary results show a large component of carbon dioxide, which would increase the vacuum pumping requirements of the entire system.

Chapter 1

Introduction

Cosmic Explorer is a next-generation observatory designed to greatly deepen and clarify humanity's gravitational-wave view of the cosmos.

Cosmic Explorer features an L-shaped geometry and houses a single interferometer. For the second site of it, each Cosmic Explore facility will have two 20 km ultrahigh-vacuum beam tubes.

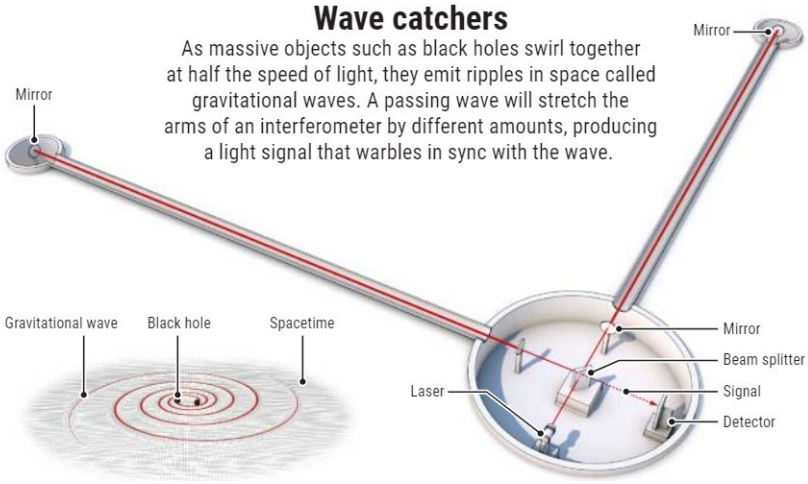

Figure 1.1: Cosmic Explorer's schematic

In the survey to attempt to build Cosmic Explorer's 20 km vacuum equipment, we want to investigate the AISI-1020 material, a low carbon steel material.

Before, scientists build two smaller detectors, using stainless steel to build pipes,

which is expensive. AISI-1020 is low-carbon steel, which is cheaper. However, the cost of vacuum equipment depends on both the cost of the pipe and the cost of the vacuum pump. The cost of a vacuum pump depends on the outgassing of the pipe, which relates to the property of the material.

For stainless steel, H_2 and H_2O will be released. An infrared laser will not interfere with H_2 but will interfere with H_2O. Our experiment starts to see how much H_2O will be released by AISI-1020. A preliminary experiment shows that after baking the pipe, the amount of gas released by the pipe will be reduced. Furthermore, we do not have H_2O released. This is a good sign. But we need further investigation on the property of AISI-1020 outgassing to see whether it can save money.

Chapter 2

Theory

The apparatus our experiment used is Fig. 2.1. The gas would come out of the AISI-1020 pipe and enter the Main Chamber through the Gate valve.

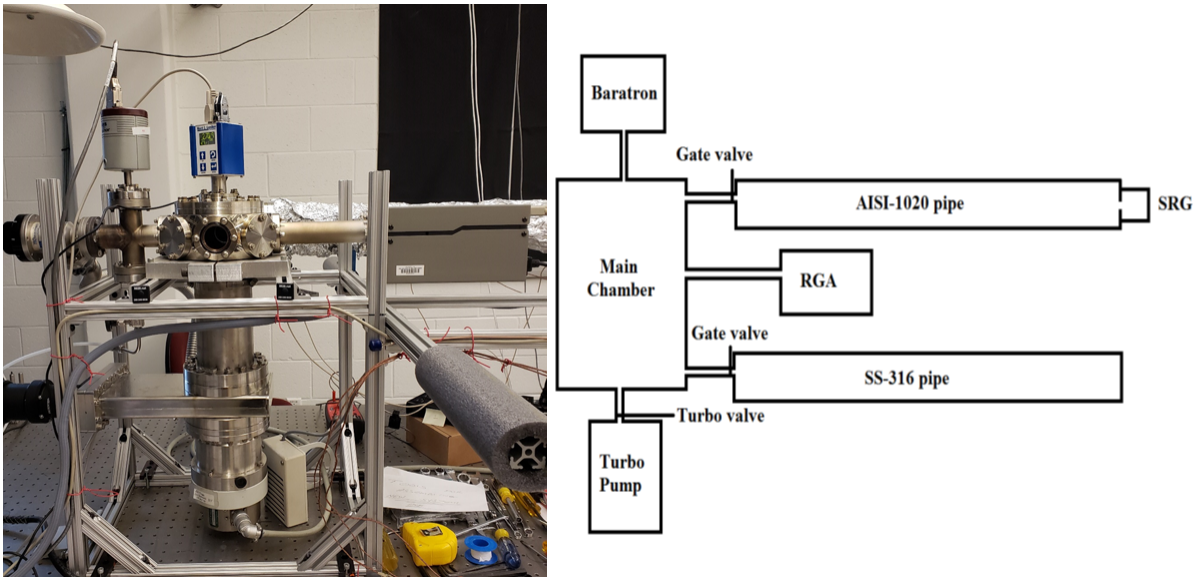

Figure 2.1: Left: Picture of the apparatus taken in the laboratory; Right: Schematic of it. Turbo Pump is used to vacuum the Main Chamber; When pumping gas out of Main Chamber, Gate valves are closed; After pumping, all valves are closed.

We first preprocess the AISI-1020 pipe before taking measurements. We bake the AISI-1020 pipe at about 400 Celsius degrees for days. The AISI-1020 pipe will thus have nearly no outgassing. Then we expose the pipe to the air. Therefore, the gas inside the pipe should be majorly air.

To investigate the property of AISI-1020 outgassing, we develop a technique to measure the amount of each composition of gas inside AISI-1020. We call this pulsed analysis technique. Firstly, Main Chamber is pumped into a vacuum by the Turbo Pump. We then begin the measurement procedure by closing Turbo (4-5 seconds) to monitor the outgassing of the main chamber. Then we open the Gate valve (for 1-3 seconds) and then close it to equilibrate pressures if we decide to release gas from the AISI-1020 pipe. Some gas will come out of the AISI-1020 pipe and enter the Main Chamber. Then we use the Residual Gas Analyzer (RGA) to observe the time-dependent signals to each selected amu (amu = [2, 18, 28, 44]) in the Main Chamber.

However, the composition of gas in the Main Chamber we analysed is not what we expect. Comparing to normal air, we see a higher level of CO_2, but a lower level of H_2O. Furthermore, since the AISI-1020 pipe and Main Chamber have the same volume (which is designed by purpose), after one pulsing of AISI-1020 gas, the pressure of AISI-1020 pipe would be halved. This means that at the second pulsing, less gas will be pulsed out of the AISI-1020 pipe and will enter the main chamber, resulting in a decrease of amount of gas. However, as shown in the Fig. 2.2, the amount of gas at the beginning of each measurement, especially of CO_2, actually steadily increases after each pulsing. Combining these two observations, we propose that some gas (especially H_2O) will stick to the wall of the Main Chamber and will not be pumped out by the Turbo Pump, which disrupts our analysis.

What's more, when we pump out gases in the Main Chamber using Turbo Pump, and leave the experimental equipment untouched, we notice that the gas amount in the Main Chamber will slowly increase, as shown in Fig. 2.3. But there should be no gas coming into the Main Chamber at this point, so the only possible source of the gas should be gas that originally sticks to the wall. It suggests the existence of

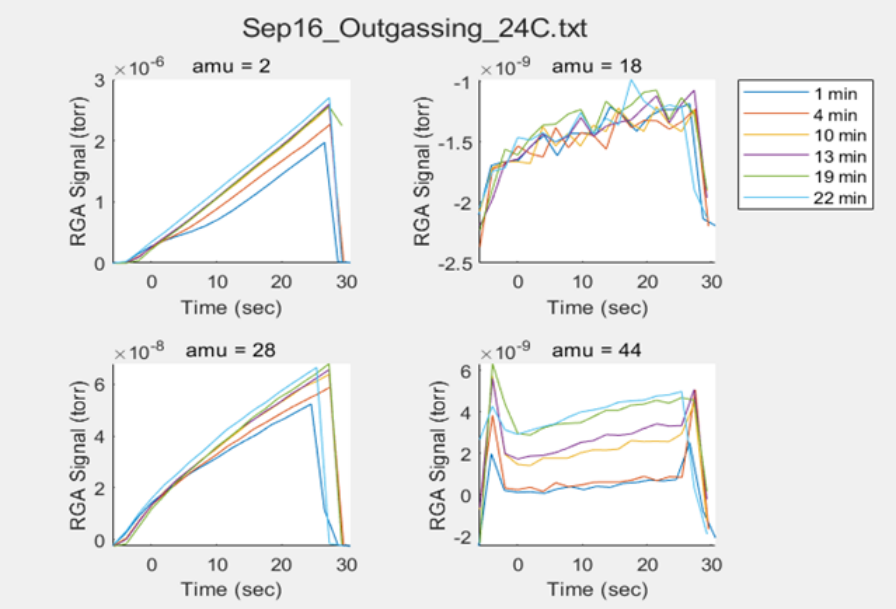

Figure 2.2: Values of RGA signal for various molecular weights, excluding measurement of pulsing. 1 min and 4 min measurements are done before the first pulsing; 10 min and 13 min measurements are done after the first pulsing but before the second pulsing; 19 min and 22 min measurements are done after the second pulsing. amu=2 is H_2; amu=18 is H_2O; amu=28 is CO; amu=44 is CO_2. The amount of gas detected, especially for CO_2, increase with after each pulsing.

stick-to-wall gas, which further reinforces our proposition.

We want to analyze the experiment data and find out numerical equations to prove our proposition and predict how long it takes for these stick-to-wall gases to vanish so that we can carry out further experiments without disruptions. To achieve this, I expect to measure parameters such as:

1. Net increase in the RGA signal value at the beginning of each measurement per amount of gas pulsed in the previous pulse

2. Net increase in the RGA signal value's increase rate per amount of gas pulsed in the previous pulse

3. The decay time for those net increases to disappear

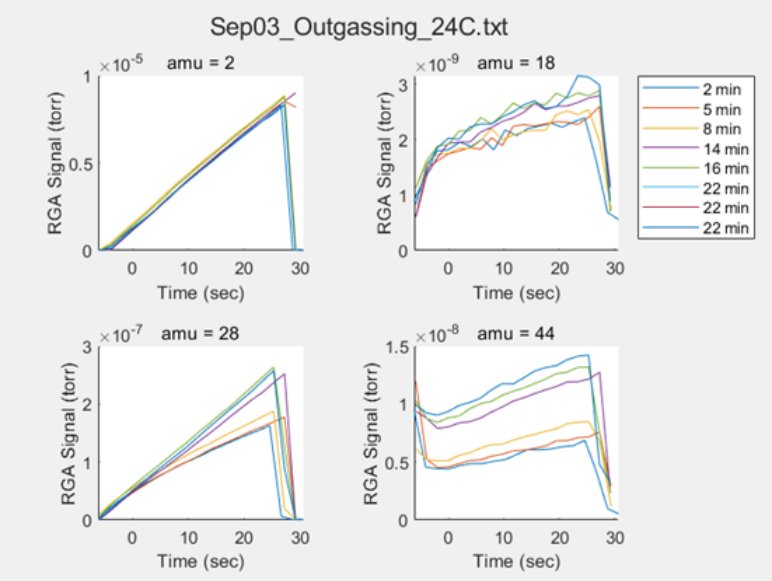

Figure 2.3: Values of RGA signal for various molecular weights, excluding measurement of pulsing. amu=2 is H_2; amu=18 is H_2O; amu=28 is CO; amu=44 is CO_2. The values, especially for CO_2, increase with time.

The first two parameters are expected to have an influence on the numerical equation since we have already observed such phenomenons as stated above. There will be further discussion on parameters in the chapter Experimental Technique.

Chapter 3

Experimental Technique

According to our proposition, the signal produced by RGA can be divided into two parts:

1. the pulsed gas from AISI-1020;
2. the gas attached to the surface of the Main Chamber during pulsing and then slowly comes out when there is no pulsing. We call it the background signal.

An example of signals collected is Fig. 3.1. Gas is pulsed at 10 min and 16 min in this example. The 10-min line, which is purple, and the 16-min line, which is blue, represent the pulsed gas value. Other lines represent the background signal value (since the pulsed value's peak is too high, other lines can be barely seen).

The background signal may come from two parts:

1. the gas attached to the surface of Main Chamber during last pulse;
2. the gas attached to the Main Chamber during previous pulses.

Under Professor Cooke's instruction, when analyzing the data, I noticed that the background signal of CO_2 changes after I let in a big pulse of the pipe, as suggested by our proposition, shown in Fig. 3.2. The gradient of the background signal of CO_2 will change significantly after a pulse.

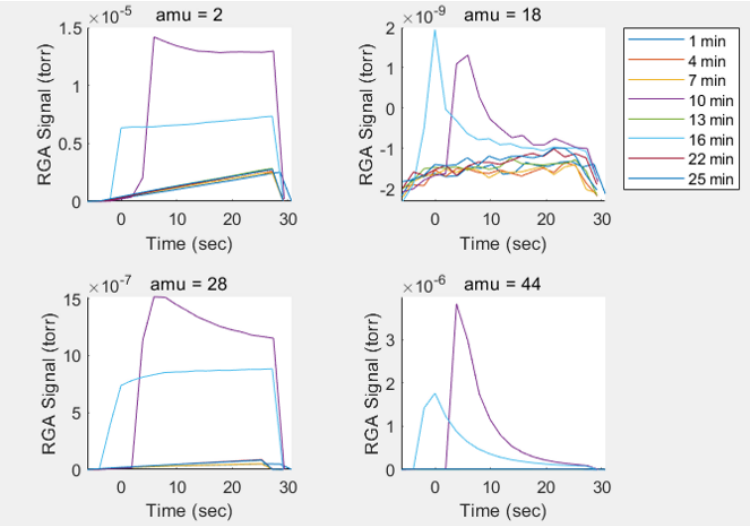

Figure 3.1: Values of RGA signal for various molecular weights, including two pulses of CO_2 (which are values of 10 min and 16 min in purple and blue color respectively). amu=2 is H_2; amu=18 is H_2O; amu=28 is CO; amu=44 is CO_2.

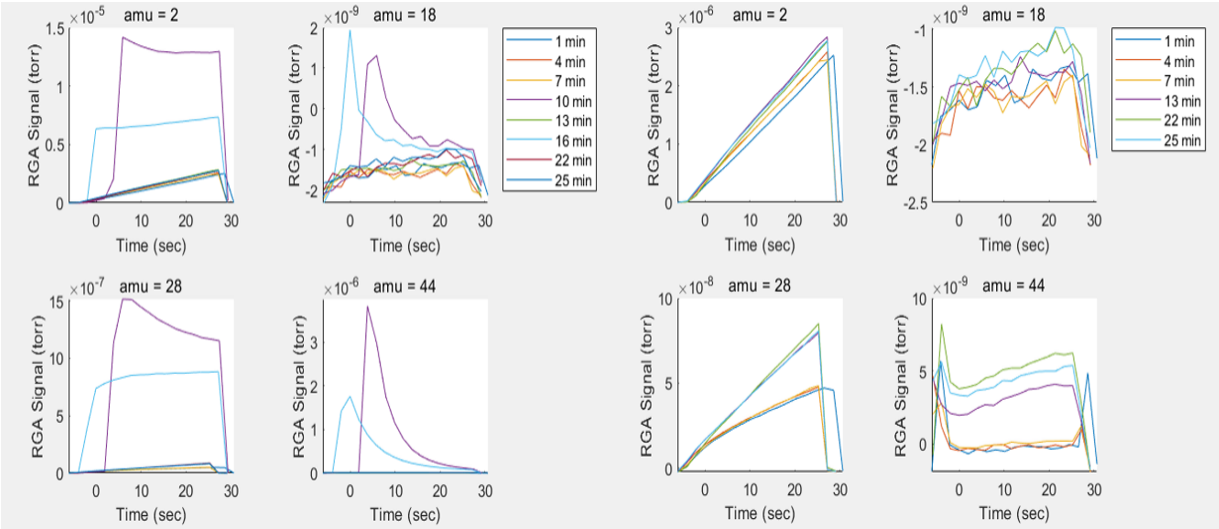

Figure 3.2: Left: Values of RGA signal for various molecular weights, including two gas pulses (at 10 min and 16 min in purple and blue color respectively). Right: Values excluding two gas pulses. CO_2's gradients change after pulses. amu=2 is H_2; amu=18 is H_2O; amu=28 is CO; amu=44 is CO_2.

Therefore, I move to analyze the relationship between the magnitude of the pulse and the gradient change of background signals. My hypothesis is such a relationship exists. Experimental data files from RGA are csv files, so I use Python and Matlab

to import and analyze them.

In the second semester, in order to find other indicators, I try to use the offset of CO_2 values before and after pulses as the indicator. An offset value is the value where the fitted line of the CO_2 background signal is at $x = 0s$. In addition, I also analyze the relationship between the magnitude of the pulse and the absolute gradient values of background signals.

Chapter 4

Results and Conclusions

4.1 Results

After two semesters investigation, our conclusions are:

1. There is a strong correlation between CO_2 pulse values and gradient changes of CO_2 background signals.

2. There is a strong correlation between H_2 pulse values and gradient changes of CO_2 background signals.

3. There is a strong correlation between CO_2 pulse values and gradients values of CO_2 background signals.

4. There is a strong correlation between CO_2 pulse values and offset values of CO_2 background signals.

5. However, there is a strong correlation between CO_2 offsets and CO_2 gradients. Therefore, we can only use one of these two parameters. Since calculated offsets have a larger error range, the gradient is a better parameter to use.

6. After the 1st pulsing, gradients will become about twice as large as before the pulsing. It seems like there is a tendency that after the 2nd pulsing gradients

will increase too. But data often overlap with each other. Without enough data here, we cannot assert that there exists such a tendency.

4.1.1 CO_2 pulse value v.s. gradient changes of CO_2 background signals

For the first conclusion, from Fig. 3.2, I came to the hypothesis that CO_2 pulses will influence the value of CO_2 gradient. To test this hypothesis, I wanted to find a correlation between the value of CO_2 pulses and the value of CO_2 gradient with reasonable variance.

To test whether this correlation exists, First I calculated the gradient from the data point collected by the RGA by fitting the best-fit line. I fitted the best-fit line with a minimum standard deviation for every line, which provides me with the gradient of each line and also the offset value. To fit the line, I only selected $0.5s$ to $20.5s$'s data value to have a better estimate of the gradient and offset. An example of best-fit lines is Fig. 4.1. The green line is the actual data collected by RGA, where red dots are the selected points used to fit. The blue line is the best fit line, which gives gradient and offset values. The blue point located around $t = 0s$ indicates the offset value. The uncertainties of fitted parameters vary. For fitted gradients, the uncertainties range from 1.2% to 34.6% mainly. For fitted offsets, the uncertainties range from 0.3% to 16.4% mainly.

Then I plotted the graph of the magnitude of the pulse vs. the gradient change of background signal, in Fig. 4.2. For some experiment trails, there exist two gas pulses. To distinguish them, I plotted them in two colors: the gradient change caused by the first pulse is colored in blue; the gradient change caused by the second pulse is colored in orange. The Sep. 6th data points, as shown in the graph, lie at an abnormal distance from other values. Therefore, we considered them outliers and

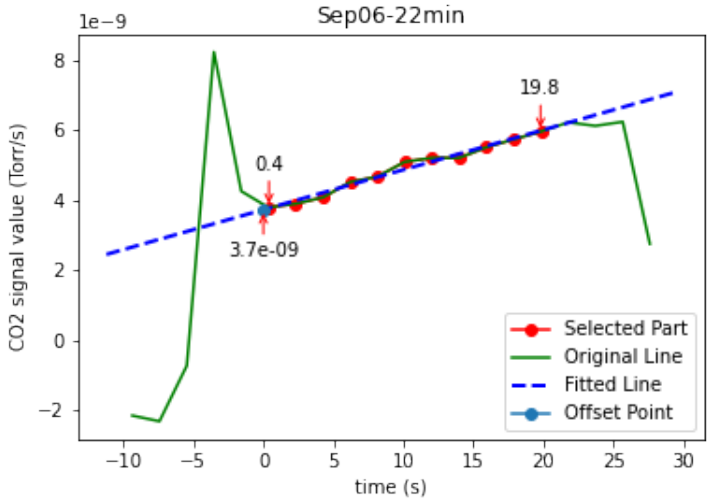

Figure 4.1: The fitted line for Sep 6th's 22min data. It is an example that shows how I fitted the data. The green line is the actual data, and the blue line is the best-fit line.

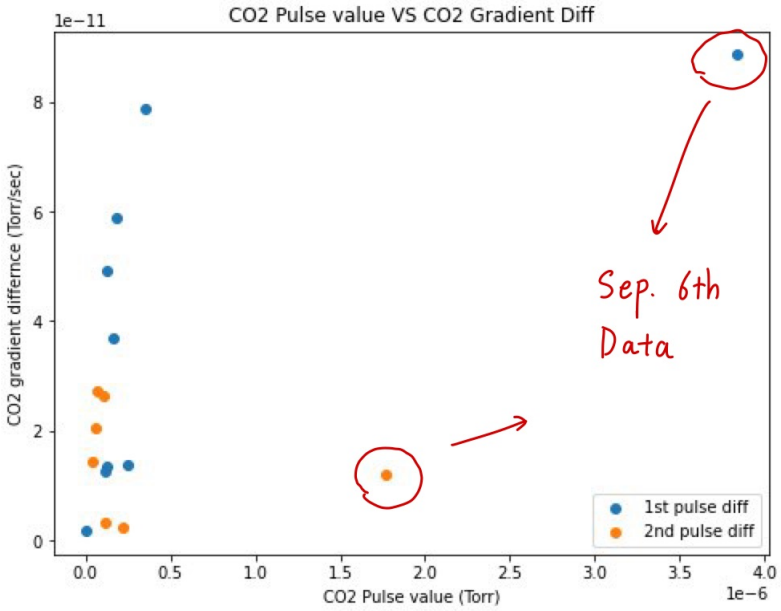

Figure 4.2: CO_2 Pulse magnitude vs. Change of CO_2 Gradient. The gradient change caused by the first pulse is colored in blue; the gradient change caused by the second pulse is colored in orange. There are two outliers from Sep.6th data.

they would be excluded.

The graph after excluding outliers from Sep. 6th is Fig. 4.3. Still, the gradient

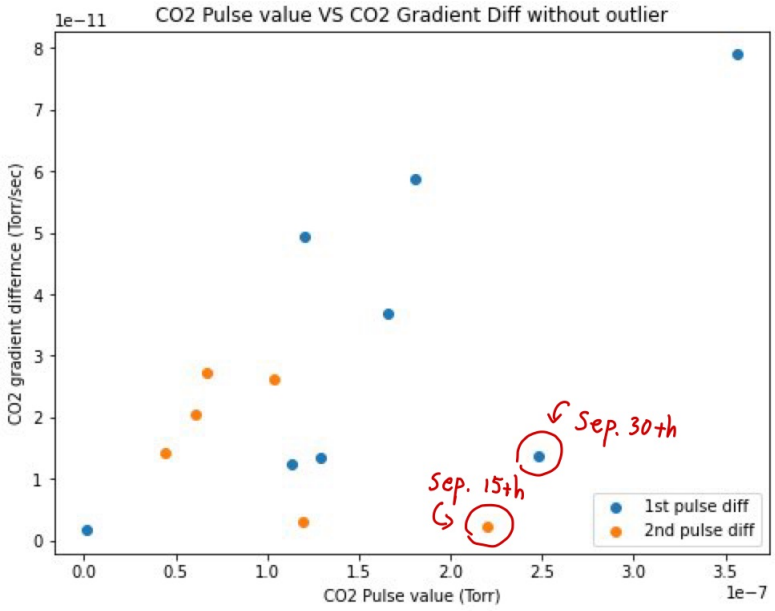

Figure 4.3: CO_2 Pulse magnitude vs. Change of CO_2 Gradient (without Sep. 6th data). There are two more outliers from Sep. 30th's first pulse and Sep. 15th's second pulse.

change caused by the first pulse is colored in blue and the gradient change caused by the second pulse is colored in orange. There are two more outliers in Fig. 4.3, as shown in the graph. The outlier of the first pulse on the lower-right side is the data from Sep. 30th; the outlier of the second pulse on the lower-right side is the data from Sep. 15th. The reasons cause these outliers remain unclear. I suspect it is due to the lack of precision when fitting the best-fit line for these two data. But further investigation is needed.

After the second exclusion of outliers, the final graph is Fig. 4.4. Again, I fitted a best-fit line, as the green straight line in the figure. The sum of squared residuals of the least-squares fit is $1.997e-21$, which is small compared to the magnitudes of the x-axis and y-axis. Therefore, we concluded that there is a strong correlation between CO_2 pulse values and gradient changes of CO_2 background signals.

However, I noticed that the initial gradients of the background signal before each

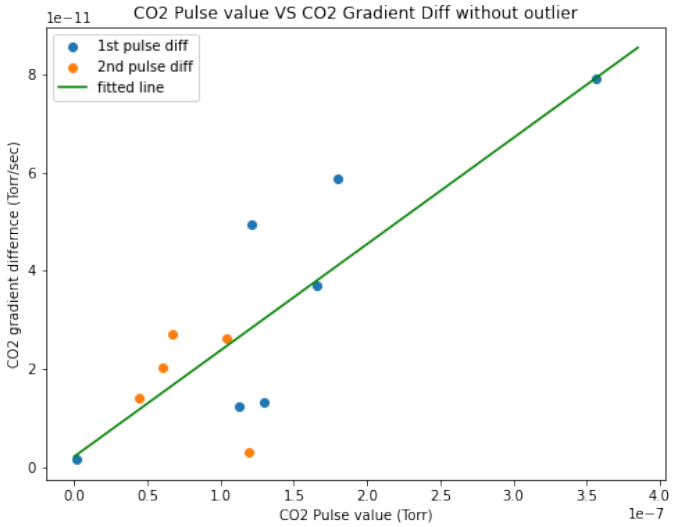

Figure 4.4: CO_2 Pulse magnitude vs. Change of CO_2 Gradient (without all outlier). The best-fit line's sum of squared residuals is $1.997e{-}21$, which is very small compared to the magnitudes of the X-axis and Y-axis. Therefore, there is a strong relationship between x and y values.

pulsing of a different date can be different, as shown in Fig. 4.5. The Y-axis of Fig.

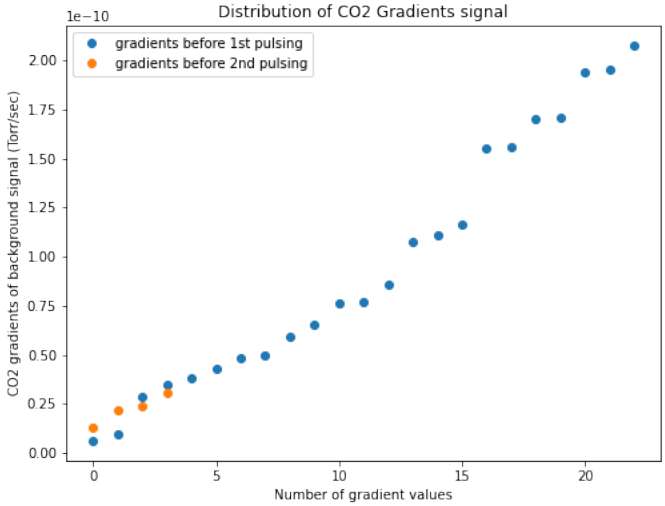

Figure 4.5: The distribution of CO_2 gradients. Y-axis indicates values of gradients (Torr/sec). Gradient values before 1st pulsing range from around $1e-11$ to $2e-10$ Torr/sec; values before 2nd pulsing range from around $1e-11$ to $3e-11$ Torr/sec.

4.5 is the value of the gradient before each pulsing of each date, which is arranged from the smallest to the biggest. Blue points are gradients before 1st pulsing, orange points are gradients before 2nd pulsing. As shown, gradient values before 1st pulsing range from around $1e-11$ to around $2e-10$ Torr/sec; gradient values before 2nd pulsing range from around $1e-11$ to around $3e-11$ Torr/sec. This shows initial gradients of the background signal before each pulsing vary in a large range.

To eliminate the influence of different initial gradients, I re-plotted the Fig. 4.4 with the y-axis changed to ratio. The ratio is calculated as the gradient value after the pulse over the gradient value before the pulse. The resulting graph is Fig. 4.6.

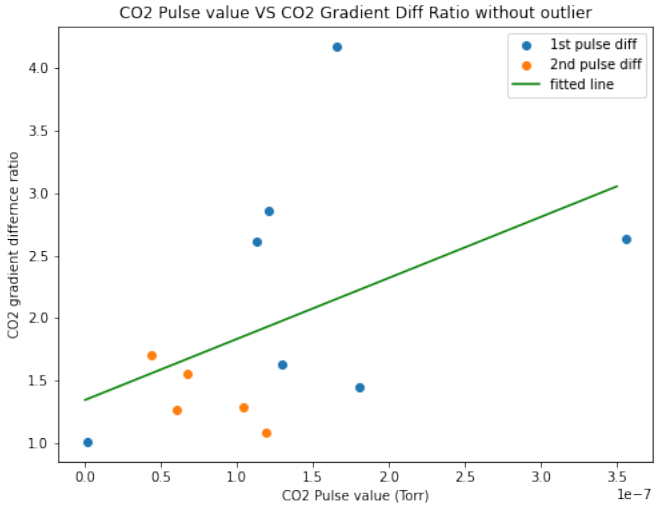

Figure 4.6: CO_2 Pulse value vs. CO_2 Gradient difference in ratio. Y-axis value is gradient value after pulsing over the gradient value before pulsing. The best-fit line's sum of squared residuals is 7.666, which is small compared to the magnitudes of the X-axis and Y-axis. Therefore, there is a relatively strong relationship between x and y values.

I also drew the best-fit line, which is the green line in the figure. The sum of squared residuals of the least-squares fit is 7.666, which is small compared to the magnitudes of the x-axis and y-axis. The relationship is still relatively strong, though

it is less strong compared to the result we got before changing the Y-axis to ratio. Thus we could safely conclude that with the influence of different initial gradients there is still a strong correlation between CO_2 pulse values and gradient changes of CO_2 background signals.

4.1.2 H_2 pulse value v.s. gradient changes of CO_2 background signals

The second conclusion is that there is a strong correlation between H_2 pulse values and gradient changes of CO_2 background signals. I investigated this with the same procedure as for the first conclusion. I excluded one more data point here, which is the value from Sep 15th's second pulse. Its pulse value is negative, which can only be explained as an error. The graph plotted after excluding outlier data and error data is Fig. 4.7. The X-axis is the H_2 pulse values, and Y-axis is the gradient changes

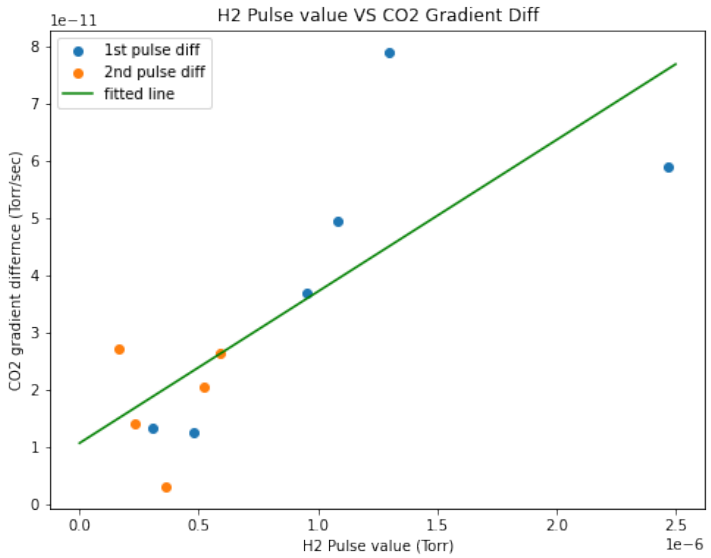

Figure 4.7: H_2 Pulse value vs. CO_2 Gradient difference. The best-fit line's sum of squared residuals is $2.152e-21$, which is very small compared to the magnitudes of the X-axis and Y-axis. Therefore, there is a strong relationship between x and y values.

of CO_2 background signals. Again, I plotted data points in two colors: the gradient change caused by the first pulse is colored in blue; the gradient change caused by the second pulse is colored in orange. The green line is the best-fit line. The graph shows there is a strong correlation too. The sum of squared residuals of the least-squares fit is $2.152e-21$, which is small compared to the magnitudes of the X-axis and Y-axis.

4.1.3 CO_2 pulse value v.s. gradient values of CO_2 background signals

The third conclusion is that there is a strong correlation between CO_2 pulse values and gradients values of CO_2 background signals. I investigated this by plotting the graph first, which is the Fig. 4.8. The X-axis is the nearest previous CO_2 pulse values, and the Y-axis is the gradients of CO_2 background signals. Gradient values directly come from the fitted line of each minute of each date (as shown in Fig. 4.1). I drew them in different colors as one color corresponding to one date, to distinguish data by date more easily. Usually, there will be 2 to 3 measurements done by RGA after one pulsing, before the next pulsing. Therefore, we can see some points have the same x values. There are three red outliers since they lie abnormal distances from other values. Outliers are still from Sep 6th.

We excluded these Sep 6th outliers, and the result is shown in the Fig. 4.9. The blue line is the best-fit line. The sum of squared residuals of the least-squares fit is $1.306e-19$, which is very small compared to the magnitudes of the x-axis and y-axis. Therefore, we could conclude that there is a strong correlation between CO_2 pulse values and gradients values of CO_2 background signals.

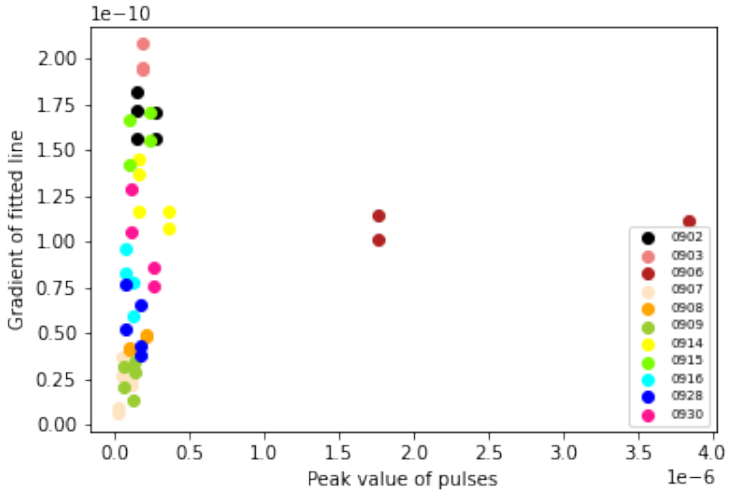

Figure 4.8: CO_2 Pulse value vs CO_2 Gradient graph. The X-axis is the nearest previous pulse value; Y-axis is the gradient value of background signals. I plotted data from different dates in different colors, to distinguish them by date faster. There are three red outliers from Sep 6th.

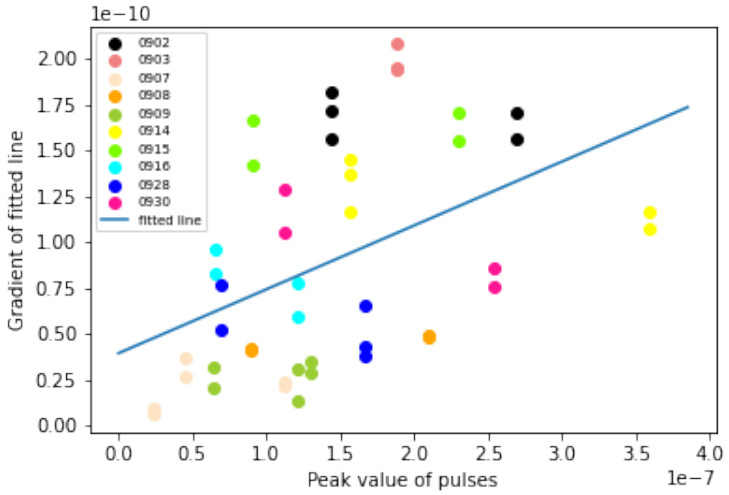

Figure 4.9: CO_2 Pulse value vs CO_2 Gradient graph, without outliers from Sep 6th. The X-axis is the nearest previous pulse value; Y-axis is the gradient value of background signals. The best-fit line's sum of squared residuals is $1.306e-19$, which is very small compared to the magnitudes of the X-axis and Y-axis. Therefore, there is a strong relationship between x and y values.

4.1.4 CO_2 pulse value v.s. offset values of CO_2 background signals

The fourth conclusion is that there is a strong correlation between CO_2 pulse values and offset values of CO_2 background signals. Similar to the procedure of getting the third conclusion, I excluded outliers from Sep 6th and plotted graph Fig. 4.10.

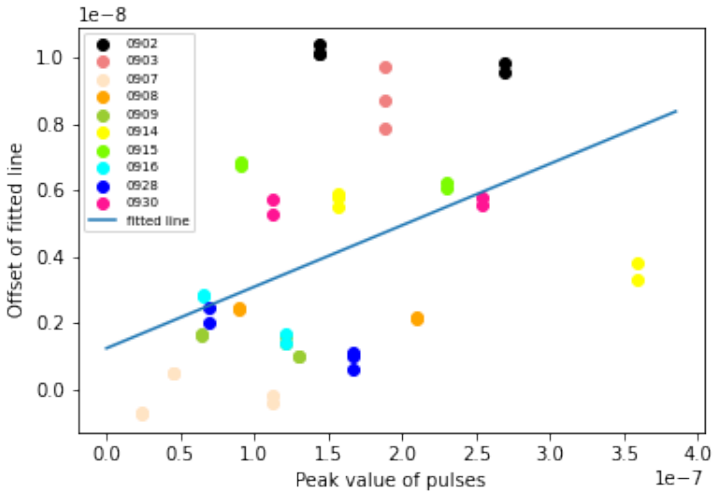

Figure 4.10: Pulse value vs offsets graph, without outliers from Sep 6th. The X-axis is the nearest previous pulse's peak value; Y-axis is the offset value of background signals. The best-fit line's sum of squared residuals is $4.056e-16$, which is very small compared to the magnitudes of the X-axis and Y-axis. Therefore, there is a strong relationship between x and y values.

The X-axis is the nearest previous CO_2 pulse values, and the Y-axis is the offsets of CO_2 background signals. Offsets directly come from the fitted line of each minute of each date (as shown in Fig. 4.1). I drew them in different colors as one color corresponding to one date, to distinguish data by date more easily. Usually, there will be 2 to 3 measurements done by RGA after one pulsing, before the next pulsing. Therefore, we can see some points have the same x values. The blue line is the best-fit line. The sum of squared residuals of the least-squares fit is $4.056e-16$, which is small compared to the magnitudes of the x-axis and y-axis. Therefore, we could conclude

that there is a strong correlation between CO_2 pulse values and offset values of CO_2 background signals.

One thing worth noticing is that Sep 6th's data produces outliers in every situation. I tried to find the reason caused this phenomenon, however, I failed to find any. There is nothing strange or special on the experiment log. But it is worth for further investigation.

4.1.5 Offset values of CO_2 background signals v.s. gradient values of CO_2 background signals

The fifth conclusion is that there is a strong correlation between CO_2 offsets and CO_2 gradients. Under Professor Cooke's instruction, I noticed that CO_2 gradients look related to CO_2 offsets. To check multicollinearity of CO_2 offsets and CO_2 gradients, I plotted the offset value v.s. gradient graph, which is Fig. 4.11. The X-axis is the CO_2 offsets, and the Y-axis is the CO_2 gradients. They both directly come from the fitted line of each minute of each date (as shown in Fig. 4.1). I drew them in different colors as one color corresponding to one date, to distinguish data by date more easily. The blue line is the best fit-line.

The sum of squared residuals of the least-squares fit is $6.530e-20$, which is very small compared to the magnitudes of the x-axis and y-axis. The graph clearly shows that these two indicators are heavily related. Therefore, I can only use one of these two indicators when trying to test the hypothesis.

However, the background signals usually do not start at exactly $t = 0s$, as shown in Fig. 4.1. Most of the time, there will be a $\pm 1s$ error. Therefore, calculated offsets have a larger error range, and the gradient is a better parameter to use.

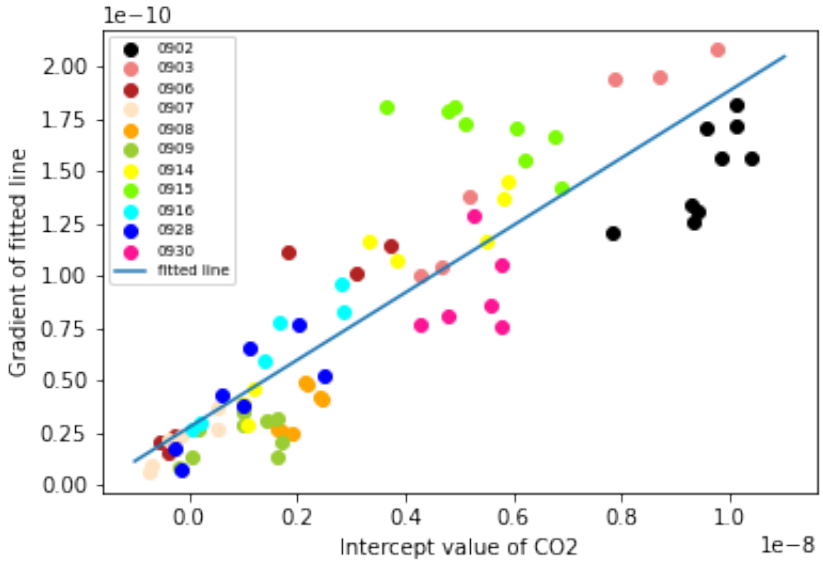

Figure 4.11: Offset vs Gradient graph. X-axis is the CO_2 offsets; Y-axis is CO_2 gradients. The best-fit line's sum of squared residuals is $6.530e-20$, which is very small compared to the magnitudes of the X-axis and Y-axis. Therefore, there is a strong relationship between x and y values.

4.1.6 Whether gradients increase after each pulsing

I noticed that it seems like the gradients after each pulsing will steadily increase. However, since the volume of the Main Chamber and AISI-1020 pipe have the same volume, the pressure inside the AISI-1020 pipe will be $\frac{1}{2}$ after one pulsing. Therefore, compared to the first pulsing, the second pulsing will only pulse $\frac{1}{2}$ of the gas out of the AISI-1020 pipe, and the gradient of CO_2 background signal should not increase. This contradicts my observation. Therefore, I decided to investigate it. I looked at the gradient values of each date and plotted graphs. An example figure is Fig. 4.12. Y-axis indicates the gradients of CO_2 background signals, and X-axis does not have meaning. Green dots represent gradients before the 1st pulsing; blue dots represent gradients after the 1st pulsing but before the second pulsing; orange dots represent gradients after the second pulsing (and before the third pulsing if there exists one on

that date). Vertical lines are error bars. The example graph shows two things:

1. After the 1st pulsing, gradients will become about twice as large as before the pulsing.

2. It seems like there is a tendency that after the 2nd pulsing gradients will increase too. But data often overlap with each other. Without enough data here, we cannot assert that there exists such a tendency.

These two conclusions work on most days. They only fail on Sep 6th, Sep 15th, and Sep 30th, which happen to be days where outliers come from.

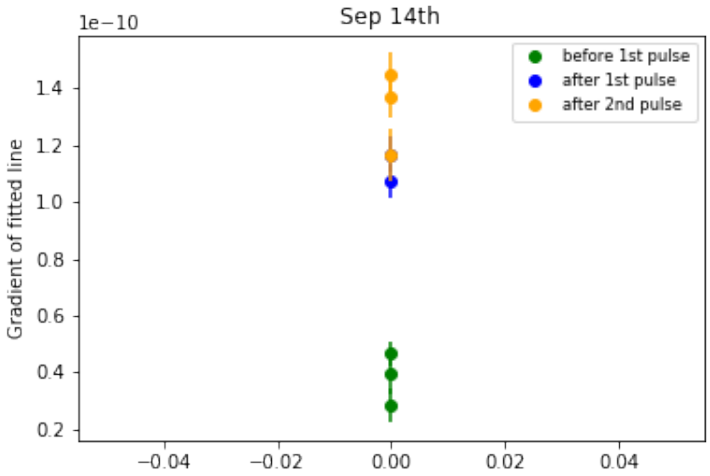

Figure 4.12: Example of how gradients change after each pulsing of Sep 14th. Y-axis indicates the gradients of CO_2 background signals, and X-axis does not have meaning. After the 1st pulsing, gradients will become about twice as large as before the pulsing. After the 2nd pulsing, data overlaps with each other. Without enough data here, we cannot assert that there exists a tendency after the 2nd pulsing.

4.2 Conclusions

In the end, I failed to reach a numerical equation to predict how long it takes for the stick-to-wall gas to vanish, but I found several significant indicators of prediction and

investigated relationships between indicators as stated above.

4.2.1 Future work

I think two major things that remain to be improved:

1. We should try to automate the pulsing of gas from AISI-1020 pipe to control the pulsing time, instead of manually operate the pulsing, in order to reduce error.

2. We should take more background signal measurements between pulses. Right now we do not have enough background signal data to determine whether gradients raise between pulses. Enough data will enable us to determine whether gradients of CO_2 background signals increase after the 2nd pulsing.

Bibliography

[1] Cosmic Explorer Website. Access: https://cosmicexplorer.org/, accessed Dec, 2021.

[2] Young, J. R. (1969). Outgassing Characteristics of Stainless Steel and Aluminum with Different Surface Treatments. Journal of Vacuum Science and Technology, 6, 398. Access: https://avs.scitation.org/doi/10.1116/1.1492700, accessed May, 2022.

[3] Richter, P. H. (1995). Estimating Errors in Least-Squares Fitting. The Telecommunications and Data Acquisition Progress Report, 42-122. Access: https://ipnpr.jpl.nasa.gov/progress_report/42-122/122E.pdf, accessed May, 2022.